

## UltraFine-Scale Structure in the Inner Corona

Richard Woo

Jet Propulsion Laboratory, California Institute of Technology, Pasadena, CA 91109

One of the most striking images of the solar corona is that of the total eclipse of 30 June 1973, enhanced to reveal a wealth and variety of ray-like structures.<sup>1</sup> Radio scattering and scintillation measurements have been combined to show that the smallest ray-like structure within coronal holes consists of flux tubes  $\sim 10^{-3}$  arcsec (1 km) at the Sun -- three orders of magnitude smaller than the smallest filamentary structure seen so far in measurements by X-rays, EUV, UV, and white-light.<sup>2-5</sup> Even smaller flux tubes pervade coronal streamers. Across the flux tubes the ray-like density structure has a spectrum that is inverse power-law with a spectral index of approximately  $5/3$  (Kolmogorov), while the spectrum of the turbulence inside the flux tubes is substantially flatter, with a spectral index near one. Confirmation of the ubiquitous ultra fine-scale coronal structure improves our understanding of the origin and evolution of interplanetary fluctuations, and makes it possible to investigate the role of small-scale coronal structure in heating and acceleration of the solar wind.

Radio observations based on scattering from electron density fluctuations, e.g., angular broadening, intensity scintillation, phase/Doppler scintillation, and spectral broadening, have served as an invaluable source of information on small-scale electron density fluctuations in the solar corona.<sup>6-9</sup> These fluctuations have generally been thought to represent random irregularities convected along the solar wind. However, imaging by X-rays, EUV, UV, and white-light have shown ray-like structure down to several arcsec scales at the Sun,<sup>2-5</sup> and recent Doppler scintillation measurements of a coronal streamer during successive solar rotations have reinforced this picture by showing long-lived

filamentary structure ranging from 1 arcmin to 1 arcsec scales and suggesting extension to sub-arcsec scales (R. Woo et al. submitted to Ap. J. Lett.).

Angular broadening is the only radio scattering measurement that can image the coronal electron density scatterers in the plane of the sky. The earliest radio interferometric measurements in the 1950s already observed scattering anisotropy that increased with decreasing radial distance, a result that was interpreted as being caused by irregularities aligned along the magnetic field and representing filamentary structure similar to the visible plumes seen in eclipse pictures.<sup>10-11</sup> Later observations confirmed this,<sup>12-15</sup> while more recent measurements with the longer baselines of the National Radio Astronomy Observatory's Very Large Array (VLA) have found that an isotropy also rises with increasing interferometer baselines (up to 35 km)<sup>16-17</sup>.

Like the larger ray-like structures observed in white-light,<sup>1</sup> the smallest filamentary structure is approximated in Figure 1 by a radially expanding flux tube. Typical 1/e level contours of the spatial electric field correlation observed by the radio interferometric measurements are drawn to illustrate that it is the size of the flux tube that limits the correlation distance transverse to the magnetic field, leading to the increase in observed anisotropy. The rise in anisotropy with decreasing radial distance or increasing interferometer baseline is hence a consequence of the growth of the size of the imaging area relative to the size of the flux tube. This means that when high anisotropies are observed, twice the correlation distance in the transverse direction would be an approximate measure of the flux tube size. Flux tube sizes based on the 1985 VLA measurements of Armstrong et al. inside  $101^{\circ} < \theta$  for which axial ratios (1/e level of electric field correlation parallel to the magnetic field over that transverse to the magnetic field) of four and greater were observed are displayed in Figure 2. The composite Solar Maximum Mission coronagraph picture reproduced from Armstrong et al.<sup>17</sup> in Figure 3, as well as the Mauna Loa coronagraph measurements during Barrington Rotation 176718, show that the east limb measurements took place over a polar coronal hole region. The results in Figure 2 show that the flux tube

is approximately 2 km at 2  $R_{\odot}$ , which when extrapolated to the Sun is 1 km ( $\sim 10^{-3}$  arcsec) with an angular size of 0.3" in heliographic coordinates.

The flux tube would be observed in scintillation measurements off the limb over a period of 0.5 sec (0.3" at the Sun's rotation rate.). Corroborating evidence for the flux tube interpretation comes from the break or inflection in the density spectrum at 5  $R_{\odot}$  shown in Figure 4, indicating a distinct change in the nature of the density fluctuations in the vicinity of the fluctuation frequency corresponding to 0.5 sec - - 2 Hz.<sup>19-20</sup> For fluctuations slower than 2 Hz, and representing the corotating spatial structure, the density spectrum is inverse power-law and Kolmogorov (one-dimensional spectral index  $\alpha = 5/3$ ), a spectrum that has been explained by some theoretical investigations.<sup>21-22</sup> For the turbulence within the flux tubes represented by fluctuations faster than 2 Hz, it is also inverse power-law but flatter ( $\alpha - 1$ ), a result that is consistent with the density spectrum deduced from the VLA angular broadening measurements<sup>17</sup>. Corresponding flux tube sizes deduced from the breaks in density spectra at 5, 10 and 20  $R_{\odot}$ <sup>19</sup> in Figure 4 are displayed in Figure 2 showing good agreement with the VLA angular scattering results.

There is further consistency in the flux tube interpretation based on the dependence of angular scattering, spectral broadening, and phase scintillation measurements on the source region at the Sun. Angular broadening measurements show an  $\sim 50\%$  increase in anisotropy from solar minimum to solar maximum,<sup>14</sup> implying that during solar maximum, when the corona is dominated by streamers and slow wind flow, the flux tubes are smaller. This is in agreement with the steepening of the density spectrum inferred from both spectral broadening and phase scintillation measurements during enhancements in scintillation<sup>20</sup> caused by coronal streamers and slow flow,<sup>23</sup> indicating a shift by a factor of 2-3 in the break of the spectrum towards a higher frequency (shorter time scale),<sup>20</sup> and hence a smaller flux tube. Thus, in the slow solar wind where the density fluctuations are high,<sup>23-24</sup> flux tubes are at least a factor of 2-3 smaller than the  $\sim 10^3$  arcsec deduced in the coronal hole region.

The spatial structure in the fast wind evolves quickly with increasing heliocentric distance, presumably because of lateral interaction of the flux tubes, as evidenced by the rapid growth in the 10 min to 5 hr time-scale density fluctuations<sup>24</sup> and the shift of the break in density spectrum to lower fluctuating frequencies observed by both scintillation and in situ measurements.<sup>25-26</sup> By 0.4 AU, the break in density spectrum has moved to about  $3 \times 10^{-4}$  Hz (-1 hr), indicating growth of the flux tubes to angular scales of  $0.5^\circ$ , consistent with the in situ observations of such structures in radially aligned measurements.<sup>27</sup> Smaller filamentary structure in the slow wind associated with coronal streamers survives to larger heliocentric distances than in the fast wind, as manifested in the Doppler scintillation measurements of coronal streamers mentioned earlier, the perseverance of the Kolmogorov density spectrum with increasing radial distance,<sup>25-26</sup> and the endurance of the high-frequency break (smaller flux tube) in the density spectrum.<sup>26</sup>

Because of solar rotation, scintillation measurements cannot observe density irregularity scales greater than a few hundred km (solar wind speed  $\times$  0.5 sec) inside, and along one flux tube, investigation of the larger scales is possible only through imaging with angular broadening measurements using baselines longer than that of the VLA.<sup>28</sup> Recent Very Long Baseline Array (VLBA) measurements of spatial scales in the 200-2000 km range did not distinguish baselines parallel (for which the spectral index  $\alpha \sim 1$ ) and perpendicular ( $\alpha = 5/3$ ) to the magnetic field, but found a spectrum that was flatter than Kolmogorov at the shorter scales, suggesting that irregularities along the flux tube were probably being observed.<sup>29</sup> The degree of anisotropy appeared to be lower with the VLBA than the VLA measurements,<sup>29</sup> which may be due to a rise in the electric field correlation in the transverse direction between flux tubes (as opposed to within) as the number of flux tubes is increased. Further studies based on VLBA measurements will clearly be useful.

The existence of corotating anisotropic structure means that velocity estimates based on multiple-station intensity scintillation measurements of fluctuation frequencies slower than about 2117 arc affected by anisotropy. Since random velocity and anisotropy produce

similar effects on intensity scintillation,<sup>30-32</sup> the conclusion that there is a turbulent (random velocity) envelope surrounding the Sun inside 15 R. based on centimeter wavelength measurements<sup>30-33</sup> may be a reflection of anisotropy instead. Meter wavelength multiple-station intensity scintillation measurements beyond 0.3 AU<sup>34-35</sup> are not affected because the flux tube size is larger there and the density fluctuations inside the flux tube are close to isotropic.<sup>36</sup> That phase scintillation and Faraday rotation fluctuations over 21 Hz are caused by corotating structures as well as large-scale irregularities convected along the solar wind is probably one of the reasons that multiple-station phase scintillation measurements do not always behave as expected<sup>37</sup> and that multiple-station Faraday rotation measurements sometimes yield negative flow velocities.~~

For over four decades, a wide variety of high-resolution spatial and temporal radio scattering and scintillation measurements have been used to probe the solar corona. The picture of an inner corona permeated by corotating filamentary fine structure unifies our understanding of these diverse but complementary measurements and explains observed features that until now have not been understood. It also confirms early ideas about the corona structure,<sup>39-42</sup> and sheds light on the nature of the compressive fluctuations observed beyond the corona.<sup>21-22, 25-26, 43-47</sup> The ultra fine-scale structure clearly represents the coronal extension of the smallest solar magnetic flux tubes that have been investigated theoretically<sup>48-49</sup> but not observed due to lack of spatial resolution<sup>50</sup>. That the inner corona comprises pressure-balanced structures means that the results from radio scattering measurements can address the important question of the role of small-scale density and magnetic structure in coronal heating and acceleration of the solar wind.

**ACKNOWLEDGEMENTS.** It is a pleasure to thank J.W. Armstrong for spirited discussion that has led to significant improvement in the paper. This paper describes research carried out at the Jet Propulsion Laboratory, California Institute of Technology, under a contract with National Aeronautics and Space Administration.

## REFERENCES

1. Koutchmy, S.P. et al. *Astron. Astrophys.* **69**, 35-42 (1978).
2. Bohlin, J. D., Vogel, S. N., Purcell, J.D., Sheeley, Jr., N. R., Tousey, R. & van Hoosier, M.E. *Astrophys. J. Lett.* 197, L1 33-1-135 (1975).
3. Habbal, S.R. *Ann. Geophys.* 10, 34-46 (1992).
4. Koutchmy, S. et al. *Astron. Astrophys.* **281**, 249-257 (1994).
- 5.13 sher, R. & Guhathakurta, M. in *Proc. of the Third SOHO Workshop - Solar Dynamic Phenomena and Solar Wind Consequences*, 447-452 (ESA SP-373, ESTEC, Noordwijk, 1994).
6. Hewish, A. in *Solar Wind* (eds. Sonnett, C. P., Coleman, Jr. P.J. & Wilcox, J.M. 477-493 (NASA Spec. pub]. 308, NASA, Washington, DC, 1972
7. Vitkevich, V.V. & Vlasov, V.I. *Astr. Zh.* 49, 595-606 (1972).
8. Colts, W. A. in *Wave Propagation in Random Media (Scintillation)*, 156-168 (SPIE, Bellingham, 1993).
9. Woo, R. in *Proc. of the Third SOHO Workshop - Solar Dynamic Phenomena and Solar Wind Consequences*, 239-248 (ESA SP-373, ESTEC, Noordwijk, 1994).
10. Hewish, A M. *N.R.S.* 118, 534-546 (1958).
11. Vitkevitch, V.V. *Astr. Zh.* 35, 52 (1958).
12. Erickson, W. C. *Astrophys. J.* **139**, 1290-1311 (1964).
13. Blessing, R.G. & Dennison, P.A. *Astr. Soc. Aust.* **2**, 84 (1972).
14. Ward, B.D. Ph.D. thesis, University of Adelaide (1975).
15. Erickson, W, C., Mahoney, M.J. & Cronyn, W.M. *B. A.A.S.* **13**, 841 (1981).
16. Narayan, R., Anantharamaiah, K.R. & Cornwell, T.J. *MNRS* 241, 403-413 (1989).
17. Armstrong, J. W., Colts, W. A., Kojima, M. & Rickett, B.J. *Astrophys. J.* **358**, 685-692 (1990).

18. Sime, D.G., Garcia, C., Yasukawa, E., Lundin, E., Rock, K., Seagraves, P.  
*NCAR/TN-274+STR*, 32-33 (NCAR, Colorado, 1986).
19. Colts, W.A. & Harmon, J.K. *Astrophys. J.* 337, 1023-1034 (1989).
20. Colts, W. A., Liu, W., Harmon, J.K. & Martin, C.L. *J. Geophys. Res.* 96, 1745-1755 (1991).
21. Higdon, J.C. *Astrophys. J.* 309, 342-361 (1986),
22. Montgomery, D., Brown, M.R. & Matthaeus, W.H. *J. Geophys. Res.* 92, 282- (1987).
23. Woo, R., Armstrong, J.W. & Gazis, P.R. *Space Sci. Rev.* 72, 223-228 (1994).
24. Woo, R., Armstrong, J. W., Bird, M.K. & Pätzold, M. *Geophys. Res. Lett.* 22, 329-332 (1995).
25. Marsch, E. & Tu, C.-Y. *J. Geophys. Res.* 95, 11945-11946 (1990).
26. Manoharan, P. K., Kojima, M. & Misawa, H. *J. Geophys. Res.* 99, 23411-23420 (1994).
27. Thieme, K. M., Marsch, E. & Schwenn, R. *Ann. Geophys.* 8, 713-724 (1990).
28. Sakurai, T., Spangler, S.R. & Armstrong, J.W. *J. Geophys. Res.* 97, 17141-17151 (1992).
29. Spangler, S.R. & Sakurai, T. *Astrophys. J.* (in the press).
30. Armstrong, J.W. & Woo, R. *Astron. Astrophys.* 103, 415-421 (1981).
31. Scott, S.I., Rickett, B.J. & Armstrong, J.W. *Astron. Astrophys.* 123, 191-206 (1983).
32. Martin, J.M. Ph.D. thesis, Stanford University (1985).
33. Ekers, R.D. & Little, L.T. *Astron. Astrophys.* 10, 310-316 (1971).
34. Rickett, B.J. & Coles, W.A. *J. Geophys. Res.* 96, 1717-1736 (1990).
35. Kojima, M. & Kakinuma, T. *Space Sci. Rev.* 53, 173-222 (1990).
36. Colts, W.A. & Kaufman, J.J. *Radio Sci.* 13, 591-597 (1978).
37. Woo, R. *Nature* 266, 514 (1977).

38. Bird, M. K., Volland, H., Efimov, A.J., Levy, G. S., Seidel, B.S. & Stelzried, C. I'. in *Solar Wind Seven* (eds. Marsch, E. & Schwenn, R) 147-150 (Pergamon Press, Oxford, 1992).
39. Parker, E.N. *interplanetary Dynamical Processes*, Interscience, New York (1963).
40. Burlaga, L.F. in *Solar Wind* (eds. Sonnett, C. P., Coleman, Jr. P.J. & Wilcox, J.M. 309-332 (NASA Spec. Pub]. 308, NASA, Washington, DC, 1972).
41. Michel, F.C. *J. Geophys. Res.* 72, 1917-1932 (1967).
42. Mullan, D.J. *Astron. Astrophys.* **232**, 520-535 (1 990).
43. Marsch, E. in *Physics of the Inner Heliosphere* Vol. 2 (eds. Schwenn, R. & Marsch, E.) 159-241 (Springer-Verlag, Berlin, 1991 ).
44. Roberts, D.A. *J. Geophys. Res.* 95, 1087- 1090 ( 1990).
45. Klein, I., W., Bruno, R., Bavassano, B. & Rosenbauer, H. *J. Geophys. Res.* 98, 7837-7841 (1993).
46. Bavassano, B. *Ann Geophys.* **12**, 97-104 (1994).
47. Tu, C.-Y. & Marsch, E. *J. Geophys. Res.* 99, 21481-21509 (1994).
48. Roberts, B. in *Physics of Magnetic Flux Ropes* (1 eds. Russell, C. T., Priest, E.R. & Lee, L. C.) 113-132 (AGU, Washington DC, 1990).
49. Thomas, J., J]. in *Physics of Magnetic Flux Ropes* (Eds. Russell, C. T., Priest, E. R. & Lcc, L. C.) 133-140 (AGU, Washington DC, 1990).
50. Stenflo, J.O. *Solar Magnetic Fields* (Kluwer, Doi drecht, 1994).

## FIGURE CAPTIONS

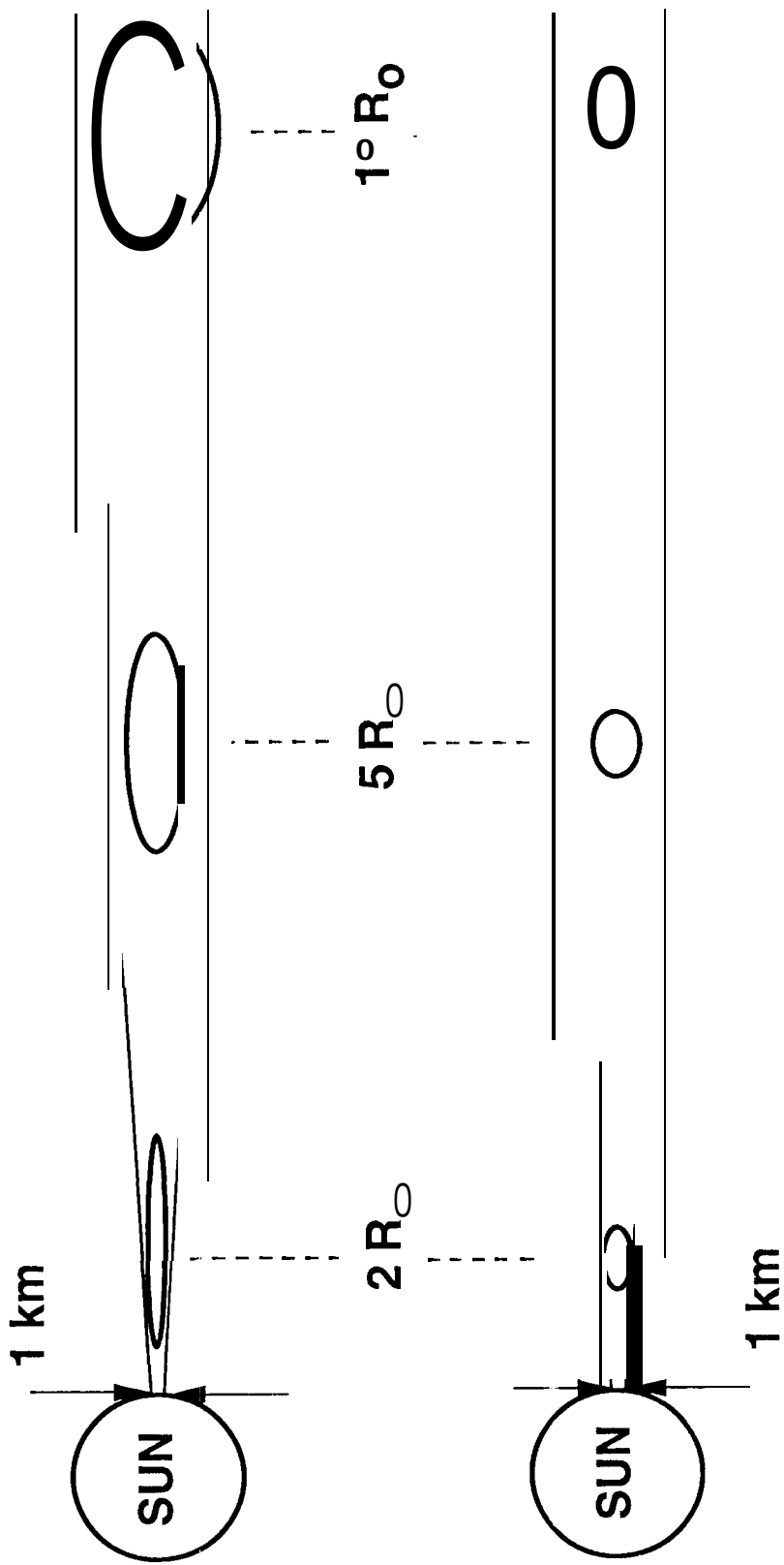
Figure 1 Schematic to illustrate how the flux tube geometry leads to scattering anisotropy observed by radio interferometric observations. The ellipses represent the  $1/\epsilon$  contour levels of the observed electric field correlation. The upper picture depicting the VLA measurements shows that the 35-km baseline (hence probing the 1-35 km scale size range) is long enough to reach the boundary of the flux tube at  $10 R_{\odot}$  leading to an axial ratio of four observed there.<sup>17</sup> Nearer the Sun, where the radial  $1/\epsilon$  expanding flux tube is smaller, the baseline reaches the boundary sooner so that a higher axial ratio of 16 is observed near  $2 R_{\odot}$ .<sup>17</sup> The lower picture, representing the 2-km baseline Culgoora measurements<sup>14</sup> that probe 0.2–2 km, shows that at a given distance anisotropy is lower in shorter baseline measurements because the measurements do not probe as close to the boundary of the flux tube. Thus, between 5-10 R. the axial ratio of the VLA measurements is 6.8 while that for the Culgoora measurements 2.3.<sup>17</sup>

Figure 2 Flux tube size as determined by twice the minor axis of the  $1/\epsilon$  contour levels of the observed electric field correlation of the 1985 VLA angular broadening measurements.<sup>17</sup> Flux tube sizes corresponding to the breaks in the density spectra inferred from phase scintillation and spectral broadening measurements at 5, 10, and  $20 R_{\odot}$  in Figure 4<sup>19</sup> are also shown. By extrapolating to the Sun assuming radial expansion, the  $2 R_{\odot}$  measurements give a flux tube size of 1 km. The measurements beyond  $5 R_{\odot}$  may be suggesting departure from radial expansion and erosion of the flux tube. When extrapolated back to the Sun assuming radial expansion, these measurements still yield flux tube sizes smaller than 5 km.

Figure 3 Composite white-light coronagraph picture taken by the Solar Maximum Mission in early 1985 October and reproduced from Armstrong et al.<sup>17</sup> The VLA measurements in Figure 2 correspond to the symbols off the east limb over the north polar coronal hole

region. The drawn lines indicate axial ratio and orientation of the major axis of the scattering irregularities and hence direction of the magnetic field. The measurements are not radially aligned, and the magnetic field direction, especially inside  $3R_{\odot}$ , is not radial but inclined towards the equator, similar to the ray structures of polar coronal hole regions observed in eclipse pictures. <sup>1</sup>

Figure 4 Model spatial spectra of electron density spectra at 5, 10, and  $20 R_{\odot}$  based on radio scintillation and scattering measurements (mainly spectra] broadening and phase scintillation) and reproduced from ref. 19. These spectra apply to transient-free conditions, and hence the fast wind<sup>23</sup>. The spatial spectra can be converted back to the original temporal spectra through multiplication by the original 1 y assumed solar wind speeds (165, 200 and 356 km/s for 5, 10, and  $20 R_{\odot}$ , respectively). <sup>19</sup> The corresponding frequencies of the vertical ticks are shown, marking the separation between the Kolmogorov spectra at lower frequencies — characterizing the flux tube structure — and the flatter spectra at higher frequencies with inner scale cutoffs — describing the turbulent structure within the flux tubes.



Figure

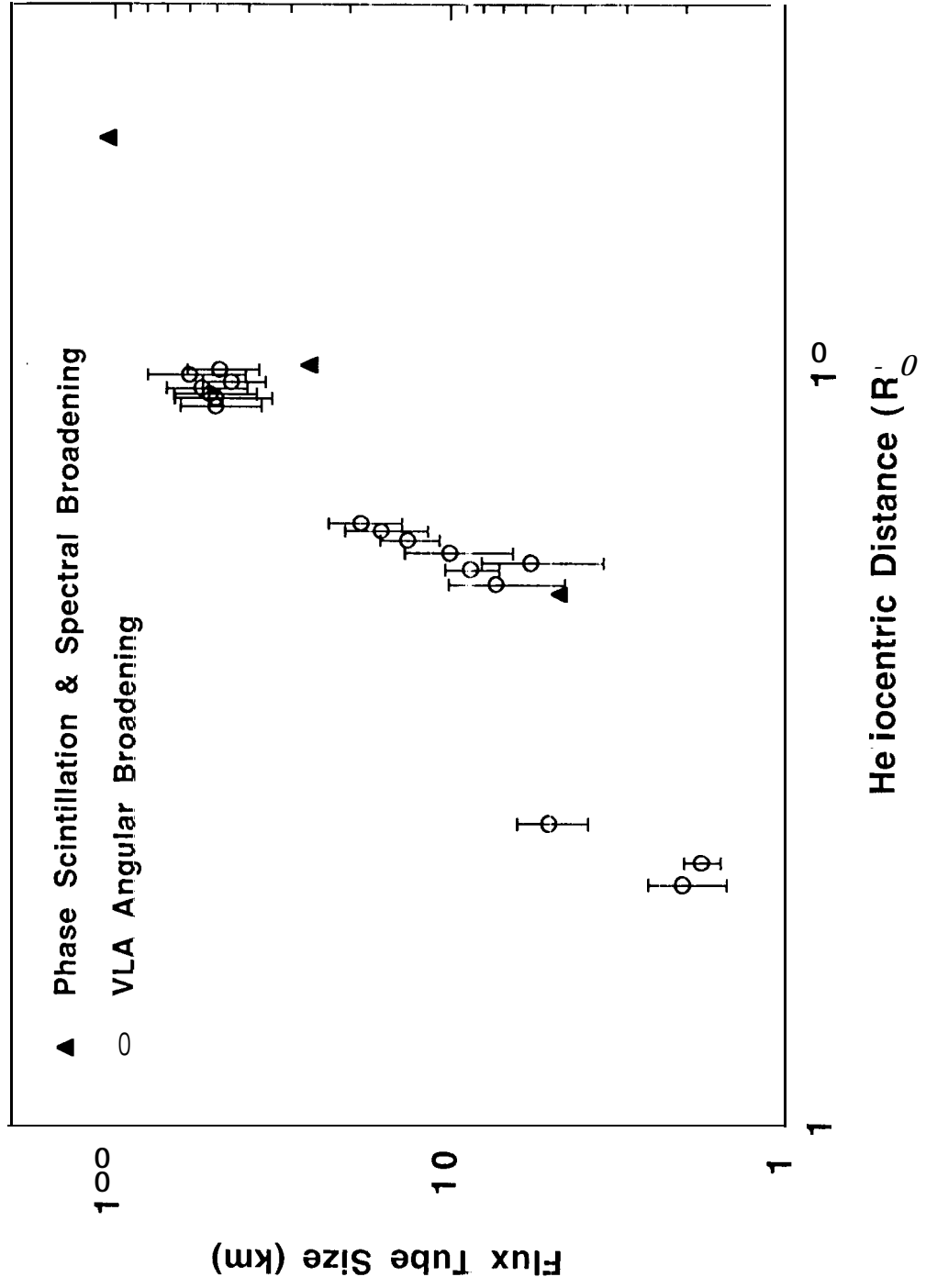


Figure 2

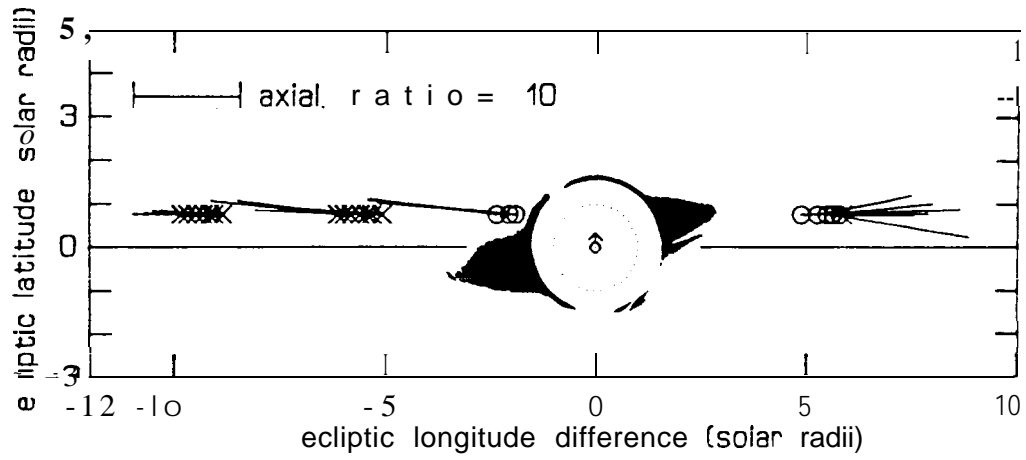


Figure 3

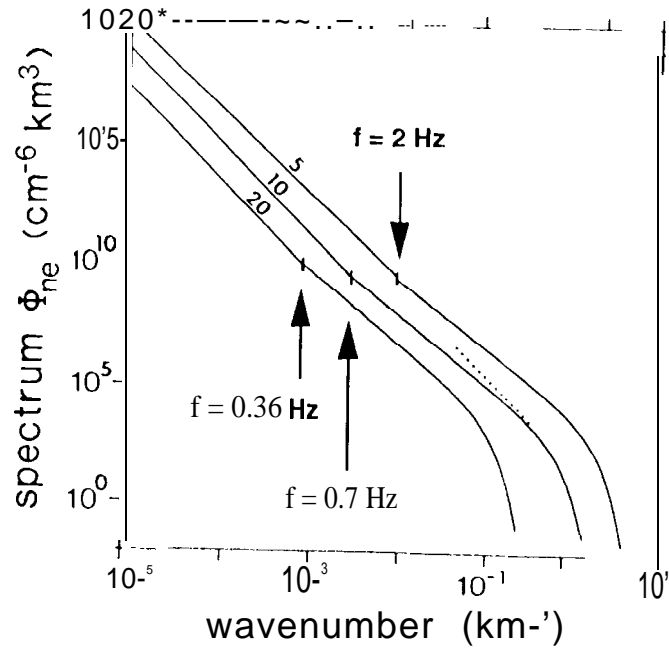


Figure 4